5-1-2018

THE MODELING, OPTIMIZATION, PRINTING, AND TESTING OF THIN-WALLED FUSED DEPOSITIONED AIRCRAFT

Nicholas Lira

THE MODELING, OPTIMIZATION, PRINTING, AND TESTING OF THIN-WALLED FUSED DEPOSITIONED AIRCRAFT

by

NICHOLAS LIRA

Presented to the Faculty of the Honors College of

The University of Texas at Arlington in Partial Fulfillment

of the Requirements

for the Degree of

HONORS BACHELOR OF SCIENCE IN MECHANICAL ENGINEERING

THE UNIVERSITY OF TEXAS AT ARLINGTON

May 2018

ACKNOWLEDGMENTS

A special thanks goes to Dr. Raul Fernandez for hosting the senior design class of 2017 – 18. Also, a thanks goes to Dr. Robert Taylor who oversaw both aircraft teams and helped guide us through the design process. The final thanks goes out to the team members of each team (AeroSpac3D: Isaac Davis, Alex Kessler, Matthew Leidlein, and Ryan Buckingham. DS WingSquad: Joakim Lea, Matt Allen, Aaron Baldride, Gavin Sabine, Jadi Yama, and Craig Conklin). Thank you for your hard work and diligence.

March 13, 2018

ABSTRACT

THE MODELING, OPTIMIZATION, PRINTING, AND TESTING OF THIN-WALLED FUSED DEPOSITIONED AIRCRAFT

Nicholas Lira, B.S. Mechanical Engineering

The University of Texas at Arlington, 2018

Faculty Mentor: Robert Taylor

The production of a 3D printed aircraft requires a procedural design and testing process to guarantee reliable manufacturing. To begin, an aircraft model is created in Computer Aided Design (CAD) software or selected from available sources. In this study, a DG-1 Version 2 model was chosen from OpenVSP, then the responsibility of production for the fuselage and wing sections were divided up into two teams. AeroSpac3D took on the fuselage, and DS Wingsquad worked on the wings. After model selection, the next step was to optimize a stiffening structure for each section in ALTAIR Hyperworks to resist forces defined by bending, torsion, tension, and pressure. The stiffening structure generated is then exported and projected on the original fuselage or wing model in CAD software. The new CAD model, with a stiffening structure, is printed, and the mechanical testing begins to validate the design procedure. In the testing phase, loads simulated in

optimization are reproduced to better understand the quality of the print and the deflections generated from loading. If failure occurs, iteration of the design must take place before printing may continue. At the time of writing this paper the wings had been printed but the fuselage had not.

TABLE OF CONTENTS

LIST OF ILLUSTRATIONS

LIST OF TABLES

CHAPTER 1

INTRODUCTION TO DESIGN AND THEORY

1.1 State of the Art

For four years, Professor Robert Taylor has worked on fused deposition manufacturing (also known as 3D printing) procedures for aircraft with students in their Senior Design Project. Dr. Taylor's primary goal in working with students is to develop a fabrication process that can translate to creating full 3D printed airplanes for industry. Currently, there are purchasable 3D printed RC planes on the market with optimized stiffening patterns for the wings. Where this project deviates from these planes that are already on the market, is in the optimization of stiffening structures for fuselages and designing joints, which allows for a more efficient transferring of loads between sections.

In past years, a single team focused on the design and printing of the wing from an airplane. For the first time in the academic year of Fall 2017 - Spring 2018, two teams signed up to work under Dr. Taylor, which allowed for the production of a full aircraft. Relying on past experience, trial and error, and guidance from Dr. Taylor, the two teams- AeroSpac3D (Fuselage) and DS WingSquad (Wing) designed a full 3D printed aircraft, which was then optimized and printed.

The 3D printer used to create the parts was the Fortus 450mc, and the printer material was a production-grade thermoplastic called ABS-M30. All of the work that went into the development of the manufacturing process described in this paper was done by undergraduate students at the University of Texas at Arlington. The design guide created

from students in past years was the most important source of information used in this project. One literature review that attempted to find information on the topic of 3D printed aircraft did not return well documented academic resources or industrial development. It appears that Airbus, a European multinational aeronautics company, has made some headway in the field. In 2016, they produced one of the first full-scale unmanned aerial vehicles (UAV) using only 3D printed parts (O'Neal). However, the methodology used was not disclosed. Furthermore, in most cases within the world of 3D printed aircraft, the planes are simple model planes. For example, 3DLabPrint, a company originally founded in Brno, Czech Republic, has fully optimized and ready to print aircraft model files that can be purchased on their website and then manufactured on local printers (3DLabPrint). Although this is exciting progress for the aerospace industry and 3D printing, 3DLabPrint is lacking the essential process of stiffening structures, which our team specializes in. Moreover, the stiffening structures implemented on the wings, seen in Figure 1.1 on the next page, look as if they were not created organically or by using optimization software. This observation can be drawn from the fact that the pattern appears periodic or standard. A comparison to the optimized stiffening pattern for the wing in this project will be drawn later to display certain advantages in using different techniques (this project used stiffening patterns generated by optimization techniques that led to a look that is more natural).

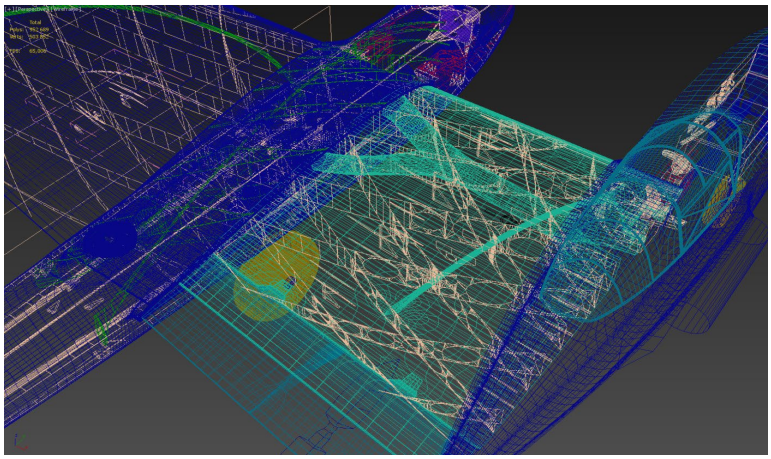

Figure 1.1: Stiffening Pattern on 3DLabPrint's Wing (3DLabPrint)

In this project, not only was there a detailed analysis on the wings to create organic stiffening patterns, the reactionary forces experienced on the fuselage were studied to develop intuitive stiffening patterns. This study led to a development in the printing process for unique types of stiffeners. To transfer loads and make up for the constraints of printer length, joints between wing and fuselage sections were designed. After the model design was completed in software, it was time to print and then to perform mechanical tests that reproduced loads that were used to create the stiffening patterns. Overall, the procedure can be summed up in a four-step process that includes: Model Selection, Topology Optimization, Printing, and Mechanical Testing.

1.1.1 Model Selection

To begin the production process, a design either needs to be created from scratch in a Computer Aided Design (CAD) software or downloaded from an open source repository. For this project, an aircraft design was chosen from OpenVSP. OpenVSP is a NASA sponsored parametric aircraft geometry tool "that allows a user to create a 3D model of an aircraft defined by common engineering parameters" (OpenVSP). It also serves as a source for engineering CAD files of aircraft that are produced by industry professionals.

For the 2017-2018 Senior Design Project, the DG-1 Version 2 was selected that can be seen in Figure 1.2. It was chosen due to its simplicity and the need to meet production goals within a one year time frame. The two important sections in this figure are the fuselage (represented by the army green) and the wings (represented by the first two and largest protruding geometries from the fuselage). The empennage, as seen on the tail end of the fuselage, was also used in this project. The aircraft propeller and the landing gear were not implemented. The length of the fuselage is 28 inches. The width of the fuselage is six to eight inches. From wing tip to wing tip, the span is 48 inches. The width of the wings is 14 inches at the base and eight inches at the wing tip.

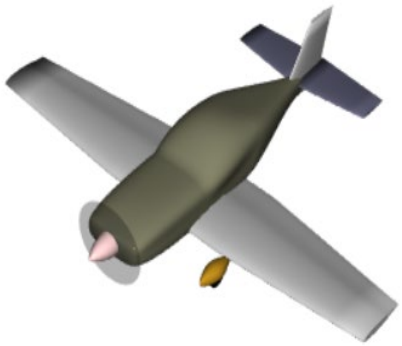

Figure 1.2: DG-1 Version 2 Aircraft for Senior Design (OpenVSP)

Once a design was chosen for the project, both teams began working on the manufacturing process for each respective section assigned to them (fuselage and wing).

1.1.2 ALTAIR Hyperworks Topology Optimization

For both the wing and fuselage bodies, the next step in producing a reliable 3D printed section was topology optimization. Topology optimization is a technique used to find optimal loading paths in arbitrary geometric models or to maximize stiffness in these

models. Stiffness is a body's capability to resist deformation when forces are applied to it. An example illustration of topology optimization is seen in Figure 1.3. In this project, Altair Hyperworks was used to do topology optimization. According to their website, Hyperworks "includes modeling, linear and nonlinear analysis, structural and system-level optimization, fluid and multi-body dynamics simulation, electromagnetic compatibility (EMC), multiphysics analysis, model-based development, and data management solutions" (About Hyperworks).

To start, certain mechanical loads (bending, pressure, tensile, and compressive) are applied to the non-optimized geometry similar to the one seen on the left. After running the computation in Hyperworks, results similar to the middle image are produced. The middle image shows the optimal amount of material needed to resist loading without mechanical failure. Finally, the optimization results are exported to a CAD software, and the original geometry is redesigned to resemble optimality, as shown in the image on the right. After optimization is complete, the printing phase begins.

Figure 1.3: Representation of the Topology Optimization Process (Bhate)

1.1.3 Printing

Of the four stages in the design process, printing is the most difficult to perform accurately. Complicated surface models need to be generated in CAD software with precise tolerancing to ensure exact prints are created. If any dimension is slightly off, the print can either print too much or too little in undesirable locations. In this case, the Fortus 450mc

printed layers were 0.02 inches thick. Therefore, any slight error in the model on the magnitude of half of the print thickness (0.01 inches) can be detrimental to the final product. To add to the challenge, there are two types of stiffeners (hat and blade) used that present unique hurdles for printing. To overcome the troubles, test prints were made in the first semester of the project to experiment with modeling techniques that would improve the printing of the fuselage and wing with their stiffening structures implemented.

The test prints were cylinders with various stiffening structures printed on the interior. These structure types are hat, blade, and hat and blade. Cross-sections of the two types of stiffener geometries can be seen in Figure 1.4. Hat stiffeners are on the right. Blade stiffeners on the left. The test prints were 2.5 inches in diameter and three inches tall. The material used for the test prints was ABS-M30 polymer, and they were printed on the University's Fortus 450mc.

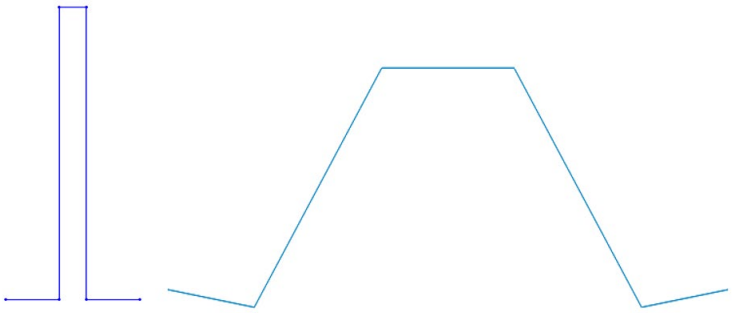

Figure 1.4: Blade (left) and Hat (right) Stiffener Cross-section Geometry

Examples of the test prints can be seen in Figure 1.5. Again, on the left are the test cylinders with blades, and on the right are test cylinders with hats.

Figure 1.5: Test Prints with All Blades (left) and All Hats (right)

Furthermore, the maximum printing height for the Fortus is 18 inches. One wing is 24 inches in length, and the fuselage is 28 inches long. This is where joint design comes into play and is necessary.

1.1.4 Mechanical Testing

Mechanical testing was performed on the fuselage and wing to reproduce loads simulated in the optimization phase. Testing is necessary because it allows engineers to determine whether the design process is a viable mode for manufacturing. If the fuselage fails or exhibits abnormal behavior during testing, iteration and further analysis will need to be performed in the design or optimization stages before printing and testing again. The same holds true for the wing. For the fuselage, only vertical and horizontal bending tests were performed. For the wing, aerodynamic pressure forces generated by the fluid dynamics of air are reproduced statically with sand bags.

CHAPTER 2

FUSELAGE

2.1 Fuselage Model

First, a brief introduction to each phase of design for the fuselage is given. In the following sections, in depth information detailing the development is given. In the academic year Fall 2017 - Spring 2018, Aerospac3D focused on the fuselage of the DG - 1 Version 2 aircraft model. Aerospac3D developed methods for finding an optimal stiffening structure within the fuselage for applied loads, fuselage joint design, printing stiffeners on thin-walled structures, and mechanical testing.

To generate a stiffening pattern, types of loadings experienced by the aircraft need to be defined. These loadings can vary depending on what the purpose of the aircraft will be. In this Senior Design Project, the loading was defined by typical maneuvers a plane carries out during flight. For example, the pitch phenomena occurs when a plane takes off and it looks as if the plane is angled upward (likewise, when it is angled downwards). Yaw is similar but for horizontal shifts. Roll happens when the plane rotates about the axis going through the center of the nose and tail. These conditions give rise to torsion (roll), vertical (pitch), and horizontal (yaw) bending. In Figure 2.1, the generated loads are shown applied to the project's model. Figure 2.1 also has the types of loads color-coded. In red, vertical bending applied at the nose and tail is shown. In blue, horizontal bending applied at the nose and tail exists. In green, torsion loading applied at the nose in the counterclockwise

direction and clockwise direction at the tail occurs. These loads are used in Altair Hyperworks to generate a stiffening pattern.

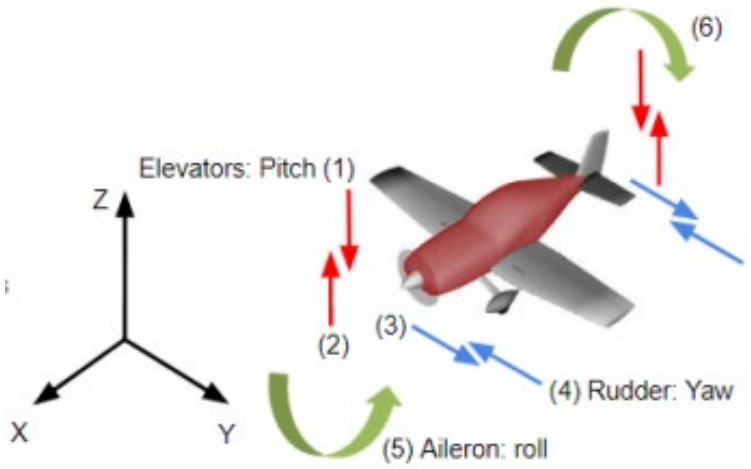

Figure 2.1: DG - 1 Model with Loads Applied to Fuselage

Recall, the length of the fuselage is 28 inches. However, the maximum printing height is 18 inches, which means that the entire fuselage cannot be printed in one session. This leads to the design and development of joints between sections of the fuselage. In Figure 2.2, the cut fuselage, representing locations for joint design, is shown. Joint design incorporates this model and is aimed at creating connections between each piece that transfers loads.

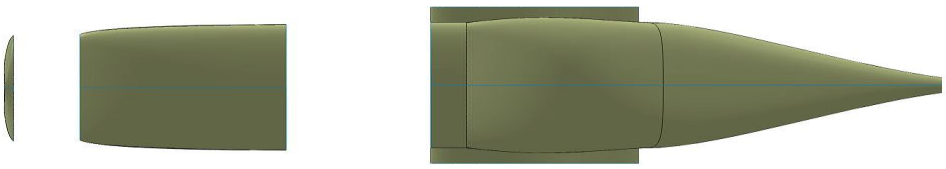

Figure 2.2: Fuselage Cut at Joints

Printing stiffeners on thin-walled structures was another challenge faced in designing the fuselage. It is particularly laborious because of the precision required to ensure that print errors do not occur. For example, the width of the print stream coming off

the Fortus 450mc is 0.02 inches, and all print models are created in such a way that they define the 'tool path.' The 'tool path' describes how the printer's tip should behave during printing. Another aspect is that the models have several surface layers so there can be two or more layers in certain regions. Issues start when layers are too close or too far apart from one another in the model. If the layers are too close, print material can bunch up and deform the print. If layers are too far away in the model, fusion between layers is weak or does not exist. Considering this, and the fact that that the work is performed under a very small order of magnitude (hundredths of an inch), it is easy to see how print errors occur and that they can be relatively frequent (if caution in modeling is not taken).

Mechanical testing for the fuselage reproduced the vertical and bending loads used in optimization. Testing of produced designs is good practice in research and industry because it validates the process. If a design fails under testing, iteration is mandatory for conclusive results.

2.2 Optimization for Fuselage Stiffening Pattern

Once an aircraft model was selected, it was time to define design loads so that a stiffening pattern could be generated in Altair Hyperworks. In this case, design loads were chosen so that they were easy to replicate using sandbags and were characteristic of typical forces experienced in flight. In Table 2.1, the types of loads applied, their magnitude, and the units used are described. Note, the English System of units are used in the calculations. To constrain the model, elements selected around the wing-fuselage interface are fixed in all degrees of freedom.

Table 2.1: Loads, Magnitude, and Units of Design Loads used for Optimization

Loads	Magnitude	Units
Counter Clock Wise Torsion at Nose	29	lbf*in
ClockWise Torsion at Tail	29	lbf*in
Horizontal Force at Nose and Tail (applied up and down)	10	lbf
Vertical Force at Nose and Tail (applied up and down)	14.7	lbf

After the magnitude of the loads were defined, the fuselage model was imported into Hyperworks and the loads were applied. This can be seen in Figure 2.3. Notice the teal colored region. This is where the fuselage is 'fixed' and cannot move in any direction. The constraints react with the forces applied.

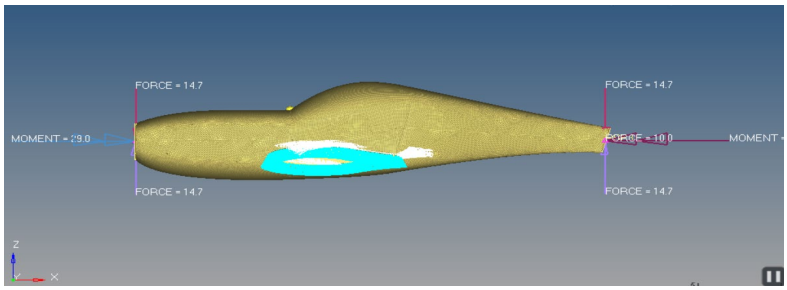

Figure 2.3: Fuselage Model with Forces Applied in Hyperworks

By setting the surface thickness of the model equal to zero and running the software, optimization results are produced. The model begins as an undefined blob then slowly converges to a discernible structure that minimizes material use and maximizes stiffness. There are additional parameters that can be tuned (for instance, the distance between stiffening members and the width of the members). Although these are interdependent, it was found that the distance between members that resulted in meaningful results was 0 - 1.5 inches, and anything above led to spare results. If the distance between members was too large and the members' width was set to be small, the optimization would

produce a sparse model with too few members. This would be a model that in reality would unlikely have the ability to withstand design loads. If distance between members is too small and the members' width is still small, extremely complex topologies that are too confusing to work with are generated. If the members are too large and spacing is small, sparse topologies are again produced but with larger members. The same occurs when the members' width are large and the spacing is large. Therefore, it is a delicate balance between each element of design. After several trial and error runs, ideal optimization results were produced as seen in Figure 2.4. The results here show a well-defined structure with good spacing of stiffeners in most regions, with a simple enough pattern that it will not be grueling to work with. In this case, the minimum distance allowed between members was set to 0 inches and the member width ranged from 0.5 to 1.5 inches. Members became too small at 0.3 inches.

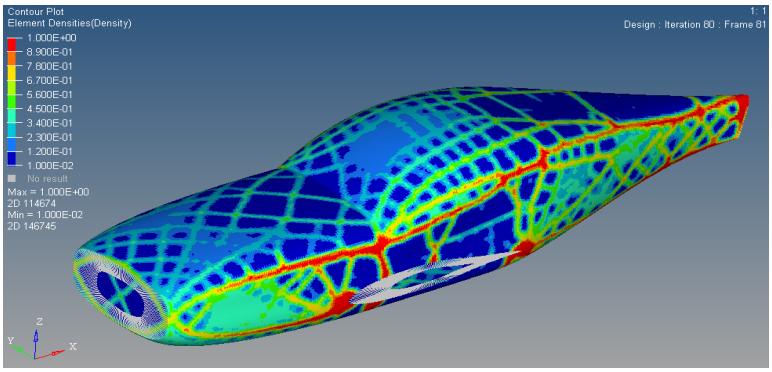

Figure 2.4: Selected Optimization Result

For these results to be useful, they are refined to include only the regions where a higher density of force is experienced. In the figure, red represents regions of high stress intensity and blue shows regions with little to none. A contour scale is located on the left hand side of the plot to illustrate these differences. Thus, only regions with higher densities

(greater than 20%) were kept to use in the design of the model. This leads to the model in Figure 2.5.

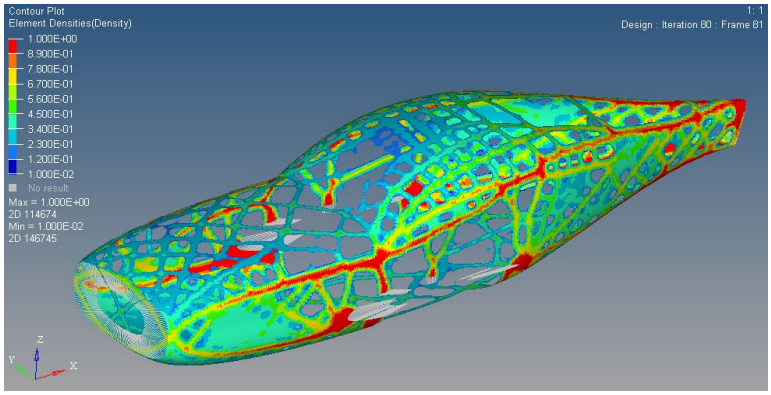

Figure 2.5: Regions of Final Optimization Used for Stiffening Structure

The model in Figure 2.5 was then exported to CAD software and implemented on the fuselage with different types of stiffeners defined based on the stress intensity modeled by optimization. For example, if the stress intensity existed below a value of 80%, blade stiffeners were used. Stress intensities of greater than 80% were implemented as hat stiffeners. The rendered version of what this looks like is shown in Figure 2.6 on the next page.

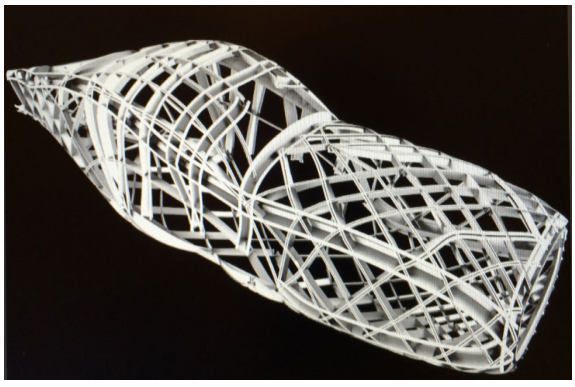

Figure 2.6: Stiffening Model Represented in CAD Software

In this figure, it is challenging to see the difference between hat and blade stiffeners. However, by comparing Figure 2.6 and 2.5 one can observe that high density regions are modeled with hat stiffeners. The same holds true for the low density regions and blade stiffeners.

2.3 Fuselage Joint Design

As discussed previously, the need for joints arises from limitations on a printer's geometric capabilities. Instead of producing bulkier and more expensive printers, a more economical approach was taken in producing smaller pieces with joints. For the fuselage, several requirements needed to be met to guarantee reliable joint interfaces. Figure 2.7, on the next page, shows the test designs for male and female joints.

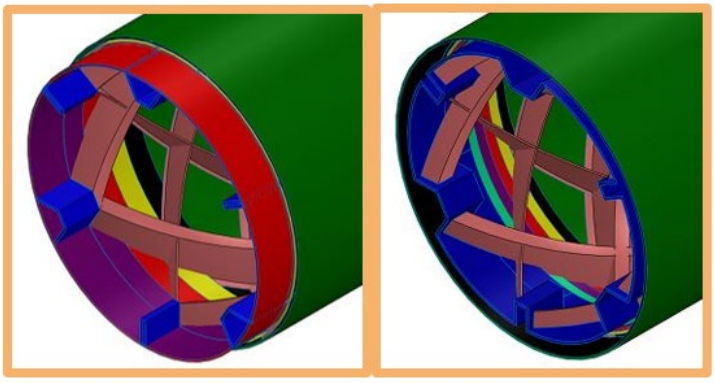

Figure 2.7: Male (left) and Female (right) Joint

Although the design procedure for these joints has not been tested yet, there are several significant design features to be implemented and considered here. Ideally, when any geometry is sliced into two pieces, the cross-sections that are mirrored along that slice will have the same area. Thus, the design of the joints becomes a problem of ensuring smooth transfer of loads between the components. In theory, this would be achieved first with a level Outer Mold Line (OML), where the skin of the two segments come together.

Next, stiffeners would be continuously placed through the joints. Theoretically, if these two aspects are met in the print, the joints will behave as desired.

Other elements of joint design that are important but do not necessarily concern themselves with the transfer of loads are printing practices. For instance, on either side of the male insert, a one bead, 0.02 inch-gap is left to guarantee quick and easy assembly. This tolerance in measurement is necessary because of the short working time when adhering the sections together. Similar design projects in the past have determined that using Super Glue is an acceptable method for fastening sections together, and by nature of Super Glue, the sections must be brought together and set in place quickly. Thus, this tolerance allows for quick insertion and accommodates for the short working time well.

Another aspect of the design is how the male joint must be implemented at the top of the print, and how the female joint must be printed at the bottom (flush with the build plate). For the male joint, this is necessary to avoid drooping along the outer mold line and ensure smoothness upon adhesion to the female. Avoiding drooping is also the reason for the female joint to be printed at the bottom.

2.4 Printing the Fuselage

The real challenge of the project existed in designing the stiffeners in CAD software so that they were able to print effectively. In past years, attempts to print the stiffeners on test cylinders resulted in awkward offsets of material that did not allow for sound structural integrity. For example, the printer would not print the base of a stiffener close enough to the outer wall that, in turn, led to weak stiffening structures.

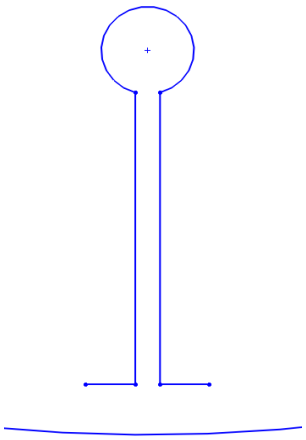

Figure 2.8: Keyhole Stiffener Next to Outer Wall

For example, a simple explanation for the CAD geometry in Figure 2.8 can be given to better understand the trouble in printing stiffeners. The curve at the bottom is the cylinder wall. The reason for not directly intersecting the wall is two-fold. First, directly intersecting the wall creates a closed shape, which will develop a seam in the stiffener. Second, it is possible to avoid having material pierce the surface of the cylinder. This is apparent once one realizes that the actual beads printed are about 0.02 inches wide. Thus, by spacing the stiffeners less than 0.02 inches away, the base of the stiffener will overlap with a portion of the cylinder wall when they are printed. When the stiffeners are woven together with the cylinder wall, a very strong connection is made. The trick is to find the optimal amount of overlap so that there is a solid connection, but not so much that the material pierces the surface of the cylinder. This exact distance is still being researched, but initial results say the ideal spacing appears to be no less than 0.01 inches.

At the time of writing this paper, the fuselage has not been printed. However, preliminary test printing on non-uniform cross-section cylinders, like that shown in Figure 2.10, have proven that the methodology works. Although the challenge becomes larger on

the actual fuselage, similar principles hold for the curves and changes in cross-sectional geometry. Therefore, it is believed that by transferring the expertise from test prints to the fuselage, successful printing will happen.

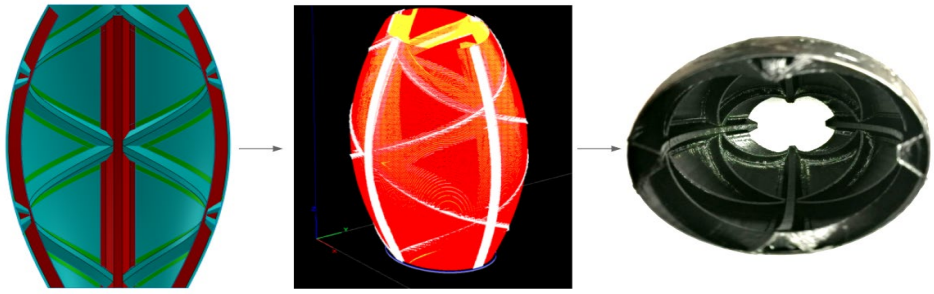

Figure 2.9: Test Printing on Non-Uniform Cross-Section Geometry

2.5 Mechanical Testing

The need to test the fuselage under mechanical loading arises out of the integrity of good practice. To reproduce the loadings from simulation once it was printed will help guarantee that a job was well done or that design efforts were productive. If the fuselage print fails under the same loads that were applied in simulation, iteration is mandatory. In this study, the loads that will be tested are the vertical and horizontal bending moments at the nose and tail.

The testing procedure will follow a four-step process:

1. Find where an equi-level plane exists. For example, two tables of the same height with a gap in between equal to a length slightly larger than the width of the fuselage, which is 6 - 8 inches.
2. From here, the fuselage will be brought to rest with its wing flanges resting on each table. Each wing flange is then secured in two places, at both ends, on the table using C-clamps. Securing the flanges tightly and at both ends will safeguard the fuselage from unwanted movement during testing. The clamps

should secure the flanges in such a way that their surface remains flush with the table at all times during testing. Deformation and movement of the fuselage should only be generated by the application of loading. To assure the fuselage is secured effectively, human-induced loads less than the magnitude of the simulated loads will be placed on the fuselage from different angles. If the fuselage is demonstrated to not slip when pushed from several defining angles, testing may commence.

3. Next comes the application of mechanical loads. To replicate the bending loads, sandbags will be placed at the fuselage nose and tail, simultaneously. Remember from Table 2.1, the force to apply at both ends is 14.7 pounds. In this application, force will be applied in increments of 5 lbs with the last application being equal to 4.7 lbs. An image from Altair is shown in Figure 2.10, which shows the loads from optimization that will be recreated for mechanical testing.

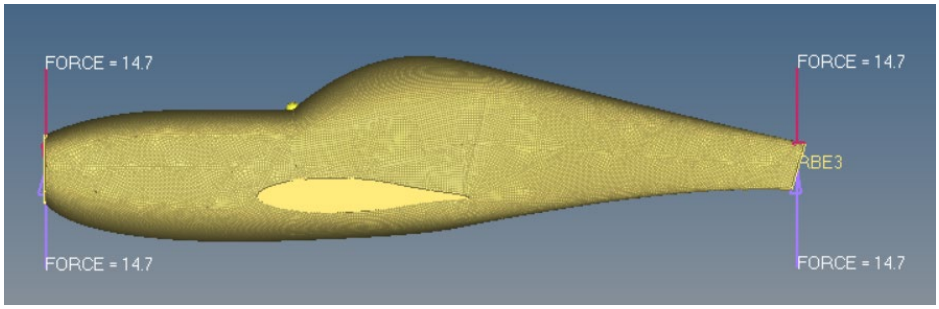

Figure 2.10: Fuselage With Up and Down Forces Applied

4. Lastly, deflection measurements will be taken at each increment of loading

CHAPTER 3

WINGS

The design and production for the wing of the DG-1 Version 2 was done by DS Wingsquad. The CAD model DS Wingsquad worked with is shown in Figure 3.1. The wing is symmetric about the fuselage, so all analysis applied to this model can be implemented for the wings on both sides. In this paper, the optimization of the wing stiffening structure, wing joint design, and mechanical testing plan for the wing will be covered. Because similar challenges existed for the fuselage, a section on the printing of the wing will be omitted. Dissimilar to the fuselage, the wing model was complete in time to print at the time of writing this paper. The printed wing weighed 0.75 lbs.

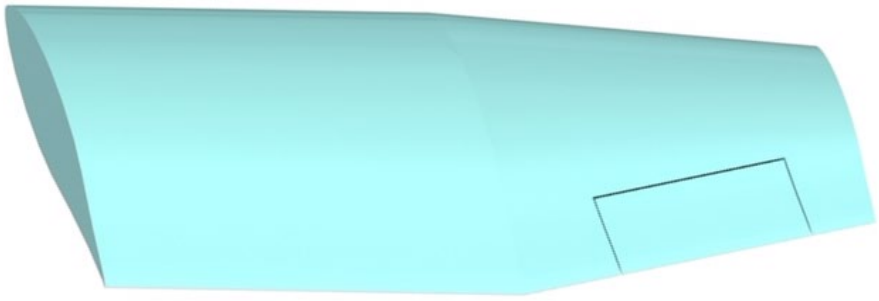

Figure 3.1: Wing CAD Model

3.1 Wing Optimization

In comparison to the fuselage, the loads experienced by the wing are significantly more complicated. This is a result of aerodynamic forces on the varying geometry of the wing. The wing experiences a different magnitude of force and bending moment depending on where pressure is applied relative to its constraint (in this case, at the point where the wing meets the fuselage). Although the same holds true for the fuselage, the wing cannot be simplified like the fuselage or inaccurate results will emerge.

The pressure on the wing was approximated to be a statically distributed load linearly decreasing from the root to wing tip, with no dynamic loading considered. The pressure is greatest where the leading edge (LE) of the wing meets the fuselage and is zero at the wing tip and trailing edge (TE), creating a quarter pyramid shape, which can be visualized below in Figure 3.2. Also, two more load cases are generated in the form of torsional loading. The remaining two load configurations account for the torsion experienced in the wing when the ailerons are deflected in the maximum up position and the maximum down position. This loading is approximated by a rectangular section of the wing near the trailing edge and wing tip to represent the aileron (refer to Figure 3.1).

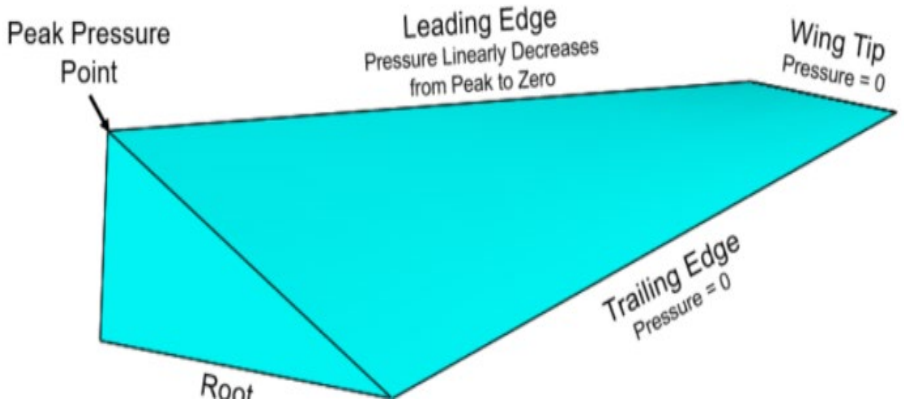

Figure 3.2: Pressure Loads Experienced by Wing

Further, each wing must carry one-half of the overall weight of the aircraft multiplied by a constant weight factor, which will be iteratively determined based on the topology optimization results (discussed later). Because this process is iterative, the weight and weight factor were normalized to a value of 1.0 in order to easily adjust the weight of the aircraft without changing other calculations. This parameterization will be assumed throughout the explanation of the load determination. The scaled weight of 0.5 pounds is distributed across the span of the wing, and ten point loads and ten torques are calculated at discretized locations across the wing to account for the distribution.

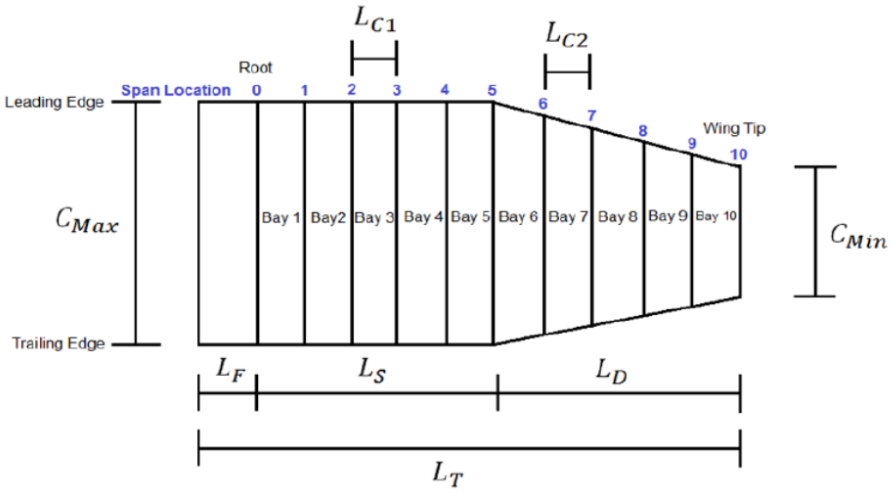

Figure 3.3: Sections of Wing Geometry Experiencing Loading

Figure 3.3 displays the top view of the wing sliced into ten bays, while Table 3.1 lists the nomenclature and values of the variables shown in the schematic. The loads are located at the quarter chord and half the width of each bay. The quarter chord is a term for the 25 percent of the chord length measured from the leading edge. Bays 1 through 5 have equal widths for the inboard straight section of the wing, while Bays 6 through 10 each have an equal width for the tapered section.

Table 3.1: Magnitude of Wing Geometries

Constant	Description	Value	Units
L_T	Total Length of Wing	24.0	inches
L_F	Half the Width of the Fuselage	3.4	inches
L_D	Length of Decreasing Section	11.0	inches
L_S	Length of Straight Section	9.6	inches
L_{C1}	Width of Bays 1 – 5	1.92	inches
L_{C2}	Width of Bays 6 – 10	2.20	inches
C_{Max}	Maximum Chord Length	8.0	inches
C_{Min}	Minimum Chord Length	5.0	inches

An excel spreadsheet was created to efficiently calculate the desired loads for each bay with the normalized weight scale. First, the maximum pressure, which is at the leading edge and root, was determined by creating a force distribution on the LE by iteration until the sum equals the desired 0.5 lbf and dividing by the area of Bay 1. From this value, the pressure on the LE at Span Location 5, the beginning of the tapered section, was calculated using a lever rule as shown in equation (1) below:

$$P_{@Span\ 5} = P_{@Root} - \left(\frac{L_S}{L_S+L_D}\right)P_{@Root} \tag{1}$$

In order to find the pressures at the remaining spans locations on the LE, the pressure differences between each span in the straight section as well as the tapered section were calculated as follows:

$$dP_{StraigHt} = \left(\frac{P_{@Root}-P_{@Span\ 5}}{5}\right) \tag{2}$$

$$dP_{Tapered} = \left(\frac{P_{Span\ 5}-P_{@Span\ 10}}{5}\right) \tag{3}$$

Using the data from the LE pressures along each span, the pressures on the LE at the middle of each bay could be easily calculated with the average of the surrounding span pressures. For example, the pressure at the middle of Bay 1 is simply the average between

the pressure at span location 0 and Span Location 1. Refer back to figure 2 for further clarity. The desired forces at the quarter chord (QC) and each mid-bay in each bay were then calculated from the equation (4) below:

$$F_{QC,Mid-Bay} = P_{LE,Mid-Bay}(L_{CHord} \cdot \frac{L_{C1\ or\ C2}}{2}) \quad (4)$$

Along with the ten forces which were calculated, the moments (torques) experienced on the wing from the pressure distribution were also approximated for the load determination process. The distance between the centroid of the pressure distribution in each bay and the quarter chord causes moments across the span of the wing. The distance was multiplied by the force at the quarter chord of each respective bay. Because of the triangular pressure distribution, the centroid of the pressure at each bay is located one third of the localized chord length from the LE. The torques at the quarter chord of each mid-bay were calculated using this equation below:

$$T_{QC,Mid-Bay} = F_{QC,Mid-Bay}(L_{TE\rightarrow QC} - L_{TE\rightarrow Centroid}) \quad (5)$$

Table 3.2 on the next page displays the forces and torques, which were calculated in each bay for the load determination. Although the table shows half of the normalized weight for the entire plane (which is five lbs), the scale factor used in Hyperworks to approximate forces was 15. This factor of 15 was used because Dr. Taylor wanted the simulated forces on the plane to represent 3-Gs (three times the gravity of Earth). The logic then follows

that a wing experiences 7.5 lbs of force in topology optimization because 15 multiplied by one half of the normalized weight is 7.5.

Table 3.2: Normalized Force Each Wing Section Experiences

Bay	Force, lb	Torque, lb-in
1	0.1044	0.0696
2	0.0857	0.0572
3	0.0842	0.0561
4	0.0581	0.0387
5	0.0639	0.0426
6	0.0391	0.0251
7	0.0423	0.0251
8	0.0138	0.0075
9	0.0043	0.0021
10	0.0040	0.0018

The aileron loading was approximated by applying a pressure distribution in both directions normal to the surface of the aileron. The aileron was represented by a rectangular cross section of 6 inches long by 2 inches wide as the rectangular section near the right side of the wing, as seen in Figure 3.1. The rectangle is located on the TE and the center of the tapered section (L_D). This magnitude of the pressure distribution was approximated to be the area of the aileron multiplied by a constant scale factor and the normalized weight of the aircraft. As with the neutral load distribution, the aileron scale factor was determined by an iterative process driven by the optimization results. Because aerodynamic systems such as this are outside of the scope of this project, using arbitrary scale factor values are not an issue. The goal is for the pressure to spread out the topology towards the aileron appropriately to simulate a reaction of an actual aileron. Adjusting the scale factors directly in HyperWorks aided greatly in the topology optimization results.

Figure 3.4: Loadsteps Used to Optimize Wing

In Figure 3.4 above, the load cases defined in Hyperworks are displayed. In Figure 3.5 below, the load cases defined are shown applied to the wing's Hypermesh model.

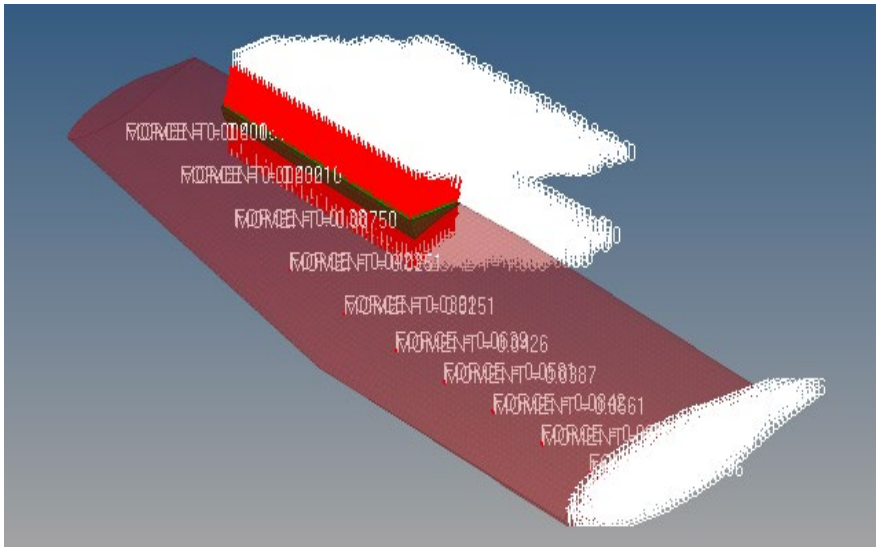

Figure 3.5: Loads Applied to Wing CAD Model

Finally, optimization results were produced for the wing. In Figure 3.6 below, an organic stiffening blueprint has been generated for the load cases. Remember the discussion on 3DPLabPrint's internal stiffening structure for the wing from the beginning of the paper and the comment made on the appearance of the stiffening structure. Notice the differences in the patterns. The wing structure from 3DLabPrint is a standardized and periodic pattern. On the other hand, the wing pattern here appears organic, created to match the exact needs of the constraints. The practical importance of this is that if the wings can

support the same amount of load using two different patterns, then the pattern with less material will save money and time in the world of 3D printing. Although this precise fact has not been proven in this paper, it is useful to tie the developments back to the real world and for competitors to understand the purpose outside the scope of Senior Design. Again, the intensity of stress experienced by a region is color coded: red for highest density, and blue for the lowest.

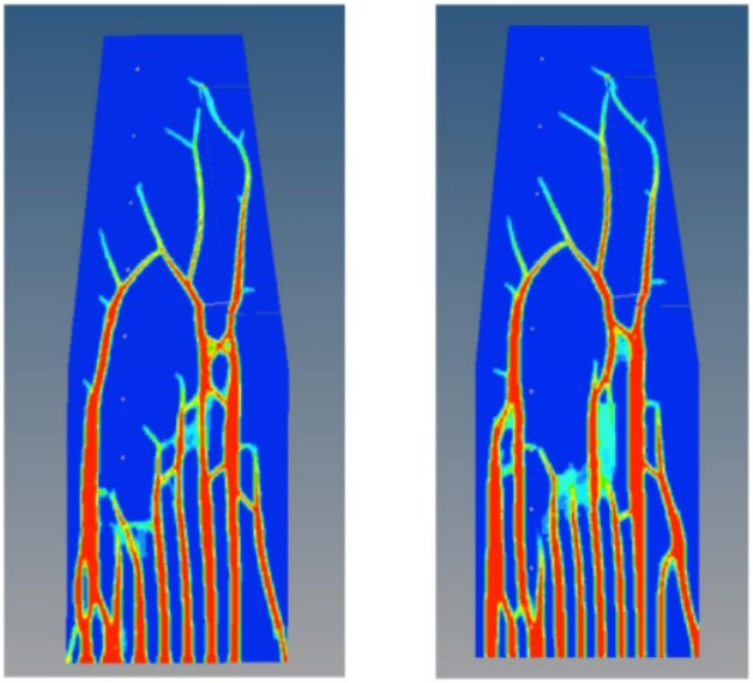

Figure 3.6: Selected Optimization Results

3.3 Wing Joint Design

Joint design for the wing was slightly less complicated than the fuselage because the complex stiffening patterns of the fuselage do not exist for the wing. Also, there are less joints to be concerned with. For example, in Figure 3.7 the two locations for the joints of the wing model are shown. One to interface with the fuselage and another designed to

compensate for how long the printer can print. That is why the second joint is placed relatively close to the center of the wing.

Figure 3.7: Locations on Wing for Joints

After the locations of the joints were determined, test prints like the models rendered in Figure 3.8 were created on the Fortus to experiment with the design and implementation. The first thing to notice is that there are two types of joints: male and female. In theory, the male joints fit smoothly into the female joints, an aspect of joint design implemented in this experiment. To ensure that the joints fit smoothly, a 0.5 - 1 bead width tolerance (bead width is 0.02 inches) is left on either side of the male joint protrusion.

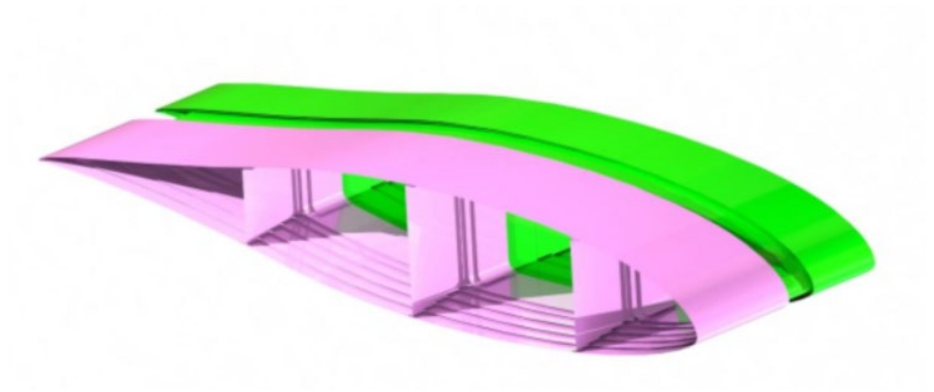

Figure 3.8: Female (pink) and Male (green) Joint Rendering

To guarantee load transfer across joints without stress concentration build up at stark changes in geometry, each type of joint is specially designed. In Figure 3.9, the female joint can be seen. The female joint is intended to have several bead layers around its

insertion to accommodate load transfer. To reduce the strength to weight ratio, c channels can be added to the mating stiffeners to reduce the required bead thickness of the lower lip. To ensure proper mating, a few key areas are important to keep in mind: the gap at trailing edge, the intersection between the stiffeners, the lower lip of the skin, and the depth of the slot. To avoid interference at the trailing edge, the lower lip of the female joint should be terminated and rounded at a sufficient distance. For this design, 0.1 inches was utilized to avoid interference. Another area of interference was the corner, where the lower lip transitions to the stiffeners. Including a .1-inch fillet helped resolve this issue. Finally, the depth of the female slot should be sufficient to ensure proper mating. A 2-3 bead tolerance proved to be satisfactory.

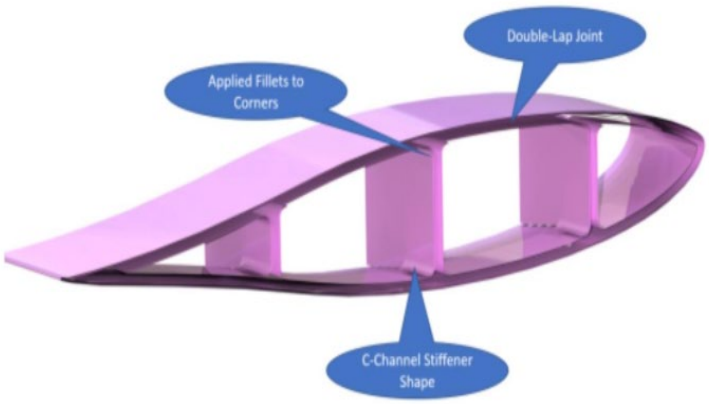

Figure 3.9: Female Joint

The male joint design, in Figure 3.10, is significantly less intricate than the female joint, and most of the areas of concern for the female joint are pertinent to the male joint as well. However, there are a few design considerations specific to the male joint. The male protrusion is recommended to be at least two beads thick; however, it can be significantly more than that. The male protrusion at the root of the DG-1 Version 2 is six beads in length.

Figure 3.10: Male Joint

3.4 Wing Testing

The same motivation for mechanically testing the fuselage exists for the wing to ensure a reliable design procedure. To test the wing, conditions simulated in the optimization phase need to be reproduced. A multistep procedure, similar to fuselage testing, was used:

1. The first step to testing the wing is to determine the nature of the loading that will be used to reproduce optimization load cases. Unlike the fuselage, a single sandbag can not be used to recreate loads. The wing experiences a pressure distribution across the entirety of its surfaces while flying. If the plane is raising in altitude, the force that is being generated on the wing by interaction with the air is known as lift. In this case, 27 sandbags were used to mimic the pressure force known as lift. Recall from the optimization section that the wing was split into ten bays. Likewise, the printed wing was sectioned off into ten sections resembling Figure 3.11. However, only Bays 2 through 10 were used because Bay 1 was submerged in the holding block. Notice the three red lines in Figure 3.11. They represent the locations at which the sand bags were placed on the wing to reproduce the pressure loading.

They are placed at 25%, 50%, and 75% of the chord length (straight line distance from the leading edge to trailing edge). The dotted lines represent the centerline for each bay, with which the sand bags were aligned.

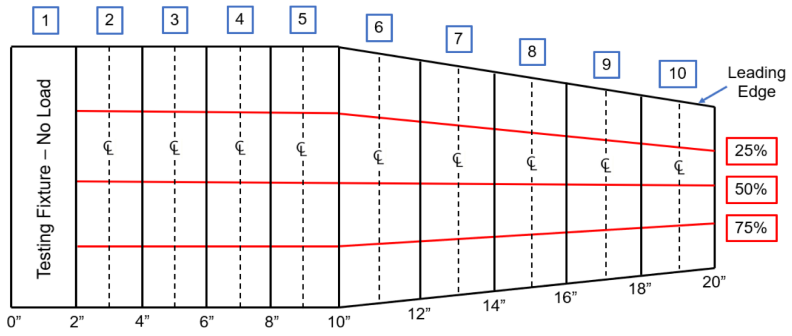

Figure 3.11: Mechanical Testing Schematic for Wing

2. Next, the amount of load and style of loading needed to be determined. For this project, a 33%, 66%, and 100% method was used. For example, the total load experienced on one wing is 5.9 lbs, excluding Bay 1 (with Bay 1 it is 7.5 lbs). Therefore, in Stage 1 of loading 33% of 5.9 lbs or 2 lbs were administered across the wing. Table 3.3 shows the magnitude of force applied at each bay for every stage. Remember there are three regions in each bay where force is applied. At the 25% mark one half of that bay's total force is applied. At 50%, one third is placed, and at 75%, one sixth. This brings Stage 2 to an end and completes the preliminary thought necessary to perform the mechanical testing. Next, details of the physical testing will be laid out.

Table 3.3: Loads Applied to Each Bay at Every Stage

		(lbs)	**33%**	**66%**	**100%**	(grams)	**33%**	**66%**	**100%**
Bay 2	0.0857		0.429	0.857	1.286		195	390	584
Bay 3	0.0842		0.421	0.842	1.263		191	383	574
Bay 4	0.0581		0.291	0.581	0.872		132	264	396
Bay 5	0.0639		0.320	0.639	0.959		145	290	436
Bay 6	0.0391		0.196	0.391	0.587		89	178	267
Bay 7	0.0423		0.212	0.423	0.635		96	192	288
Bay 8	0.0138		0.069	0.138	0.207		31	63	94
Bay 9	0.0043		0.022	0.043	0.065		10	20	29
Bay 10	0.004		0.020	0.040	0.060		9	18	27
	SUMS	5.9	2.0	4.0	5.9		898.6	1797.3	2695.9

3. A sand bag static loading test was chosen as the most effective and simplest method for the test to be performed. Before the test can be conducted, a testing structure needs to be designed such that the wings can be placed in the structure without allowing the wing to move except in a natural downward deflecting manner. A configuration similar to the one DS WingSquad used is shown in Figure 3.12. During testing, the white block that is being held was firmly secured using two C-clamps. However, to reproduce the lift loads experienced in flight, it was flipped upside down.

Figure 3.12: Testing Configuration for the Wing

4. Once the wing and holding block were securely fastened, sandbags were applied. Figure 3.13 shows the wing with sandbags for the 33% load configuration.

Figure 3.13: Wing with Sandbags

In Table 3.4 the deflections for each stage of loading are summarized. The initial and final deflection is the measurement from the wing tip directly to the ground. A point was

established on the ground directly beneath the wing tip in order to reduce error in subsequent deflection measurements. Stage 1 initial deflection is deflection without any load, while the final deflection has 33% of the load applied. But the initial deflection for Stage 2 is with 33% of the load applied (i.e. the final deflection of Stage 1); the same is true for Stage 3.

Table 3.4: Deflections of Wing Under Loading

Stage	Initial Deflection (in)	Final Deflection (in)	Change in Deflection (in)
1 (33% of load)	$36\frac{1}{32}$	$35\frac{31}{32}$	$\frac{1}{16}$
2 (66% of load)	$35\frac{31}{32}$	$35\frac{29}{32}$	$\frac{1}{16}$
3 (100% of load)	$35\frac{29}{32}$	$35\frac{26}{32}$	$\frac{3}{32}$

Ultimately, the printed wing withstood all design loads, which validates DS WingSquad's print. The final deflection was 0.22 inches. The wing weighed in at approximately 0.75 lb, meaning both wings combined weighed 1.5 lbs. With the expectation that the fuselage would weigh about 2 lbs, the estimation of a 5 lb aircraft was a little high, yet the wing surpassed expectation in mechanical testing. Further testing could be conducted on the wing, if time permitted, to test the wing to failure. Judging by the stiffness of the wing, it might be able to sustain double the design load, or more, fairly comfortably. But of course, more testing would be needed to validate this hypothesis. Future work would include cleaning up the STL file by removing duplicate layers. This would ultimately decrease weight of the aircraft, improve surface finish, and increase stiffness to weight ratio.

CHAPTER 4

CONCLUSIONS

In this paper, the process in which the DG-1 Version 2 was taken from a simple CAD rendering to a 3D printed aircraft was described. Two Senior Design Teams, AeroSpac3D and DS WingSquad, took on the fuselage and wings of the DG-1, respectively. In their work they found and optimized stiffening structures for loading resistance, designed joints out of compensation for printer constraints, and printed the original plane with the stiffening structure and joints implemented.

By the end of the teams' second semester, each section had been optimized and fully implemented in CAD so that printing could commence. At the time of writing this paper, the wing had been successfully printed and tested. Only the fuselage remains unprinted. Although the year of Senior Design is coming to an end, it is still the intention of both teams to completely produce and test one iteration of the plane. Indeed, a combined effort from both teams is being put forth to partake in the 2nd Annual 3D Printed Aircraft Competition hosted by the University of Texas at Arlington. Overall, the progress made broke new ground for Dr. Taylor's vision of enhancing the manufacturing process and mechanical reliability of 3D printed aircraft.

REFERENCES

3DLabPrint, 2018. https://3dlabprint.com/.

"About Hyperworks." *Altair Hyperworks,* 2018. https://altairhyperworks.com/About-Hyperworks.

Bhate, Dhruv. "Additive Manufacturing - Back to the Future." *PADT*, 28 January 2016, http://www.padtinc.com/blog/additive-mfg/additive-manufacturing-back-to-the-future.

O'Neal, Bridget. "Airbus Officially Unveils Thor, The Fully 3D Printed Plane that Flies Beautifully." *3DPrint,* 6 June 2016, https://3dprint.com/137389/airbus-thor-3d-printed-plane/.

OpenVSP, 2018. http://openvsp.org/.

BIOGRAPHICAL INFORMATION

Nicholas Lira studied Mechanical Engineering and Mathematics at the University of Texas at Arlington (UTA). After his sophomore year, he spent a year in Germany at the Brandenburg University of Technology. Upon his return from Germany, he began working with the High Energy Physics (HEP) group at UTA. With the HEP group, he collaborated on the Deep Underground Neutrino Experiment (DUNE) where he studied the effect of geometric uncertainties of the magnetic field horns on the pion flux and the 3x1x1 ProtoDUNE Liquid Argon Time Projection Chamber.

Nicholas is particularly interested in entrepreneurism. In 2015, he served as an undergraduate fellow at the University of Texas at Austin's IC Squared Institute. Currently, he works for AnomalousDL, a startup focused on developing deep learning consulting. He has developed his own business models but decided to finish school before attempting to start a business.

If his entrepreneurial interests pan out, he does not think he will go back to school. However, if they do not or he decides to continue learning in an academic environment, he plans on going to graduate school for data science.